Defective autophagy in vascular smooth muscle cells increases passive stiffness of the mouse aortic vessel wall

Defective autophagy in vascular smooth muscle cells increases passive stiffness of the mouse aortic vessel wall

Dorien G. De Munck, Arthur J.A. Leloup, Guido R. Y. De Meyer, Wim Martinet, Paul Fransen

Laboratory of Physiopharmacology, University of Antwerp, Antwerp, Belgium

Corresponding author: Paul Fransen, Laboratory of Physiopharmacology, University of Antwerp, Universiteitsplein 1, 2610 Antwerp, Belgium

tel.: (+32)32652917, e-mail: paul.fransen@uantwerpen.be

ORCID ID :

Dorien G. De Munck : 0000-0002-5506-5392

Arthur J.A. Leloup : 0000-0003-2014-3618

Guido R. Y. De Meyer : 0000-0003-3848-8702

Wim Martinet : 0000-0003-1967-9343

Paul Fransen : 0000-0002-4577-3416

Abstract

Aging and associated progressive arterial stiffening are both an important predictor for the development of cardiovascular diseases. Recent evidence showed that autophagy, a catabolic cellular mechanism responsible for nutrient recycling, plays a major role in the physiology of vascular cells such as endothelial cells and vascular smooth muscle cells (VSMCs). Moreover, several autophagy inducing compounds are effective in treating arterial stiffness. Yet, a direct link between VSMC autophagy and arterial stiffness remains largely unidentified. Therefore, we investigated the effects of a VSMC-specific deletion of the essential autophagy related gene Atg7 in young mice (3.5 months) ($Atg7^{F/F}$ SM22α-Cre^{+} mice) on the biomechanical properties of the aorta, using an in-house developed Rodent Oscillatory Tension Set-up to study Arterial Compliance (ROTSAC). Aortic segments of $Atg7^{F/F}$ SM22α-Cre^{+} mice displayed attenuated compliance and higher arterial stiffness, which was more evident at higher distention pressures. Passive aortic wall remodeling, rather than differences in VSMC tone, is responsible for these phenomena, since differences in compliance and stiffness between $Atg7^{+/+}$ SM22α-Cre^{+} and $Atg7^{F/F}$ SM22α-Cre^{+} aortas were more pronounced when VSMCs were completely relaxed by the addition of exogenous nitric oxide. These observations are supported by histological data showing a 13% increase in medial wall thickness and a 14% decrease in elastin along with elevated elastin fragmentation. In addition, expression of the calcium binding protein S100A4, which is linked to matrix remodeling, was elevated in aortic segments of $Atg7^{F/F}$ SM22α-Cre^{+} mice. Overall, these findings illustrate that autophagy exerts a crucial role in defining arterial wall compliance.

Keywords: Autophagy, vascular smooth muscle cell, arterial stiffness, mouse aorta

1 Introduction

Autophagy is an evolutionary conserved process involved in the degradation and recycling of cytoplasmic constituents. In basal conditions, autophagy is necessary to maintain cellular homeostasis by ensuring the turnover of aged or damaged proteins and organelles. Basal autophagy can be rapidly upregulated upon stress conditions to promote cell survival [8, 28]. Moreover, autophagy determines the lifespan of many organisms [13], hence dysregulation of this process is associated with the development of age-related cardiovascular disorders including heart failure, atherosclerosis, hypertension and arterial stiffness [7, 31, 32]. Increased arterial stiffness is identified as an independent predictive value for cardiovascular diseases and mortality [34, 40].

Recently, we demonstrated that autophagy is important for the regulation of Ca^{2+} homeostasis and contractility of vascular smooth muscle cells (VSMCs) [25]. Specific deletion of the essential autophagy gene Atg7 promotes overexpression and enhanced depolarization of the voltage gated calcium channels. In addition, the Ca^{2+} store capacity of the sarcoplasmic reticulum increases, which results in higher inositol 1,4,5-triphosphate (IP_3)-mediated Ca^{2+} release upon phenylephrine activation. Because autophagy deficient VSMCs reveal cellular hypertrophy, increased levels of collagen and an elevated migration capacity, autophagy also has major implications for the VSMC phenotype [12]. These effects in turn can influence the aortic extracellular matrix (ECM), which is an important passive modulator for arterial stiffness [41]. Research with autophagy inducers has shown that there is a potential link between impaired autophagy and arterial stiffness [17, 19]. However, these studies focus on endothelial cell (EC) dysfunction and oxidative stress as a mechanism by which enhanced autophagy improves arterial stiffness, but they fail to provide a link between autophagy in VSMCs and vascular stiffness. Given that both EC and VSMC function contributes to stiffness of large arteries [21], and autophagy deficiency affects Ca^{2+} homeostasis of VSMCs, in this study we determined the functional and biomechanical properties of vessel segments of mice with a deletion of the essential autophagy gene Atg7 in VSMCs using a Rodent Oscillatory Tension Set-up to study Arterial Compliance (ROTSAC) [20]. Since the main purpose of this study was to define the role of

autophagy in arterial stiffness, we focused on determining biomechanics of the aorta because this is the most important vessel with (patho)physiological relevance concerning this matter. As such, we could directly investigate the effects of VSMC autophagy on arterial stiffness, which were assessed at different wall pressures and different levels of VSMC and EC stimulation. In addition, underlying structural and morphological differences were determined by histological analysis.

2 Material and methods

2.1 Mice and tissue preparation

Mice on a C57BL/6 background and with a selective Atg7 gene deletion in VSMCs ($Atg7^{F/F}$ SM22α-Cre^{+})[26] as well as wild-type littermates without the Atg7 deletion but expressing SM22α-Cre ($Atg7^{+/+}$ SM22α-Cre^{+}), were housed in the animal facility of the University of Antwerp in standard cages with a 12:12h light-dark cycle and had access to regular chow and water ad libitum. At the age of 3.5 months, animals (both male and female) were euthanized by perforating the diaphragm after anesthetizing with pentobarbital sodium (250 mg kg^{-1}, i.p.). The thoracic aorta was carefully isolated and stripped from adherent tissue. Starting from the diaphragm, the descending thoracic aorta was cut into segments of 2 mm length (5 segments). Two segments of each mouse were mounted in a horizontally oriented oscillating organ bath to study biomechanical properties. Data represent the average of these two vessel segments. $Atg7^{F/F}$ SM22α-Cre^{+} and $Atg7^{+/+}$ SM22α-Cre^{+} mice were dissected in parallel. Vessel segments were immersed in Krebs Ringer (KR) solution [containing (in mM) 118 NaCl, 4.7 KCl, 2.5 $CaCl_2$, 1.2 KH_2PO_4, 1.2 $MgSO_4$, 25 $NaHCO_3$, 0.025 CaEDTA and 11.1 glucose; pH 7.4] at 37°C and continuously aerated with 95% O_2/5% CO_2. All animal procedures were approved by the ethics committee of the University of Antwerp.

2.2 Rodent Oscillatory Tension Set-up to study Arterial Compliance (ROTSAC)

Ex vivo vascular stiffness was determined via ROTSAC measurements as previously described [20]. In brief, aortic vessel segments were mounted in organ chambers (8 ml) between two wire hooks and segments were continuously stretched between alternating preloads corresponding to the 'systolic' and 'diastolic' transmural pressures and at a physiological frequency of 10 Hz to mimic the physiological heart rate in mice

(600 beats/minute). At any given pressure, calibration of the upper hook allowed calculation of the diastolic and systolic vessel diameter (mm), the compliance (µm/mmHg) and the Peterson modulus (Ep). Ep was defined as the pulse pressure [difference in pressure (ΔP), which was 40 mmHg in the present study], multiplied by the diastolic diameter (D_0), and divided by the diameter change (ΔD) between diastolic and systolic pressure, or $Ep=D_0*\Delta P/\Delta D$. Contraction and relaxation of vessel segments were elicited as described above.

2.3 Echocardiographic evaluation

Transthoracic echocardiograms were acquired in anesthetized mice (1.5-2.5% isoflurane v/v; Forene, Abbvie) using a high frequency ultrasound system (Vevo2100, Visualsonics) while maintaining heart rate at 500±50 beats/min and body temperature between 36-38°C. M-mode images were obtained for LV function evaluation. Ejection fraction (EF), left ventricular mass (LVmass) and stroke volume (SV) were calculated using measurements of three consecutive M-mode cycles.

Pulse wave velocity (PWV), which is an in vivo measurement of arterial stiffness, was measured according to a method developed by Di Lascio et al. [9] in the abdominal aorta and using a 24-MHz transducer. Briefly, the aortic diameter (D) was measured on 700 frames-per-second B-mode images of the abdominal aorta in EKV imaging mode. Hereafter, pulse wave Doppler tracing was used to determine aortic flow velocity (V). The ln(D)-V loop method was then applied to calculate PWV using Mathlab v2014 software (Mathworks).

2.4 Histology

Vessel segments were fixed in 4% formalin for 24 hours and paraffin embedded. Transversal sections were stained with haematoxylin-eosin (H&E), orcein or Sirius red to determine wall thickness, elastin and collagen content, respectively. The number of VSMCs was quantified by determining the number of nuclei in the media between the internal and external elastic lamina. Elastin fragmentation was quantified in a blinded manner by counting the number of interruptions in the elastin fiber and expressed as number of elastin breaks per aortic section. S100A4 was assessed by immunohistochemistry using anti-S100A4

(DACO, A5114) monoclonal antibody. Images were acquired with Universal Graph 6.1 software using an Olympus BX40 microscope and quantified with Image J software.

2.5 Western blot analysis

Vessel segments were lysed in Laemmli sample buffer (Bio-Rad) containing 5% β-mercaptoethanol. Samples were heat-denatured for 5 minutes and loaded on Bolt 4-12% or 12% Bis-Tris Gels (Life Technologies). After gel electrophoresis, proteins were transferred to Immobilon-FL membranes (Merck Millipore) according to standard procedures and incubated for 1 hour in Odyssey Blocking Buffer (LI-COR Biosciences). Next, membranes were incubated at 4°C overnight with the following primary antibodies: mouse anti-LC3B (Nanotools, clone 5F10, 0231-100), rabbit anti-SQSTM1/p62 (Sigma-Aldrich, P0067) or mouse anti-β-actin (Sigma-Aldrich, A5441). Finally, membranes were incubated with fluorescently-labeled secondary antibodies to allow IR-detection on an Odyssey SA instrument (LI-COR Biosciences).

2.1 Statistics

All data are expressed as mean±SEM with n representing the number of mice. Statistical analysis was performed using Graphpad Prism software (version 8.3.0). Statistical tests are mentioned in the figure legends. $p<0.05$ was considered as statistically significant.

3 Results

3.1 Autophagy is defective in aorta segments of $Atg7^{F/F}$SM22α-Cre^{+} mice

Western blot analyses of aorta segments from $Atg7^{F/F}$ SM22α-Cre^{+} mice revealed typical features of autophagy deficiency such as the absence of essential autophagy protein Atg7, the accumulation of the autophagy substrate p62 and a decreased conversion of the soluble isoform LC3-I to the autophagosome associated LC3-II (Figure 1).

3.2 Autophagy deficiency in VSMCs decreases aortic compliance at high distention pressures

Aorta segments of $Atg7^{F/F}$ SM22α-Cre^{+} and $Atg7^{+/+}$ SM22α-Cre^{+} mice were immersed in Krebs Ringer solution and subjected to transmural pressure steps of 40 mmHg at different diastolic (40 up to 260 mmHg)

and systolic (80 up to 300 mmHg) pressures. Next, the pressure-dependency of the diastolic diameter (D_0), compliance and Peterson modulus (E_p) from an average distention pressure of 60 mmHg (40-80 mmHg) to 280 mmHg (260-300 mmHg) were measured. Segments of $Atg7^{F/F}$ SM22α-Cre^+ showed a lower compliance between 120 and 240 mmHg and a higher Ep at distention pressures between 120 and 220 mmHg as compared to $Atg7^{+/+}$ SM22α-Cre^+ control mice (Figure 2).

To evaluate whether increased basal tonus is responsible for these differences, VSMCs were completely relaxed by addition of 2 μM exogenous NO donor (DEA NONOate (DEANO)), which caused a small, but significant increase of diastolic diameter in both strains and at all pressures (Figure 3). The increase in diastolic diameter was larger at intermediate pressures than at low or high pressures (Figure 3A). As expected, full relaxation with DEANO increased compliance of the segments (Figure 3B, positive values) whereas Ep was decreased (Figure 3C, negative values). At the highest transmural pressure, the change in compliance or stiffness by relaxing the segments with DEANO was negligible. The attenuated diastolic diameter and compliance, as well as the elevated stiffness of $Atg7^{F/F}$ SM22α-Cre^+ mice as compared to $Atg7^{+/+}$ SM22α-Cre^+ mice, were not reversed by DEANO ($p<0.05$ for genotype factor with D_0 , $p<0.01$ for genotype factor with Ep, $p<0.001$ for genotype factor with compliance). This indicates that passive vessel wall remodeling is responsible, at least partially, for differences in diameter, compliance and Ep in aortic segments of $Atg7^{F/F}$ SM22α-Cre^+ mice. Overall, effects of arterial relaxation through exogenous NO on diameter, compliance and stiffness were smaller in $Atg7^{F/F}$ SM22α-Cre^+ VSMCs as compared to $Atg7^{+/+}$ SM22α-Cre^+ VSMCs (Figures 3A, B and C).

Previously, we showed that α_1 adrenoceptor stimulation of VSMCs with PE causes a decrease in diameter and compliance and an increase in stiffness [21]. In the present study, VSMC contraction was initiated in aortic segments of both $Atg7^{F/F}$ SM22α-Cre^+ and $Atg7^{+/+}$ SM22α-Cre^+ mice by the addition of 2 μM of PE (Figure 4). PE-induced constriction resulted in changes of diastolic diameter, compliance and stiffness, and these changes were pressure-dependent. The diastolic diameter was only decreased between pressures of 100 to 260 mmHg, compliance was decreased below pressures of 160 mmHg and stiffness was increased

up to pressures of 160 mmHg. At higher pressures, compliance was barely affected (Figure 4B), while stiffness decreased (Figure 4C). The decrease of compliance or increase of stiffness by PE turned to negligible changes of compliance or de-stiffening at lower pressures in $Atg7^{F/F}$ SM22α-Cre^{+} versus $Atg7^{+/+}$ SM22α-Cre^{+} aorta segments (Figure 4B).

To avoid the interference of basal NO release with the effects of PE, the abovementioned experiments were repeated after addition of the eNOS inhibitor L-NAME (Figure 5). Inhibition of basal NO shifted the differences in compliance between $Atg7^{F/F}$ SM22α-Cre^{+} and $Atg7^{+/+}$ SM22α-Cre^{+} aortic segments to 180-280 mmHg and differences in Ep to 180-260 mmHg (data not shown), while differences at lower distention pressures disappeared. Similar to contraction with PE, a significant interaction could be observed between the genotype and pressure with the magnitude of the effect of compliance (Figure 5B).

Subsequently, we studied pressure-dependency of $Atg7^{+/+}$ SM22α-Cre^{+} (Figure 6A-B) and $Atg7^{F/F}$ SM22α-Cre^{+} segments in control and stimulated conditions (Figure 6C-D). Although no difference in absolute effect of PE or PE with L-NAME was observed between the two groups, a significantly lower x-intercept and a trend towards a lower x-intercept with the effects of PE (Figure 6E) and PE with L-NAME (Figure 6F) was seen in $Atg7^{F/F}$ SM22α-Cre^{+} mice as compared to $Atg7^{+/+}$ SM22α-Cre^{+} mice. This indicates that the pressure at which the magnitude of PE and PE with L-NAME changes direction is significantly lower in $Atg7^{F/F}$ SM22α-Cre^{+} mice.

3.3 Autophagy deficiency in VSMCs induces extracellular matrix remodeling

To investigate vessel wall remodeling responsible for the difference in passive arterial stiffness observed in the ROTSAC setup, histological analysis was performed on the most important vessel wall components. Medial wall thickness, measured on an H&E staining of the aorta, was significantly increased in $Atg7^{F/F}$ SM22α-Cre^{+} mice as compared to $Atg7^{+/+}$ SM22α-Cre^{+} mice. This increase was not due to an increase in the number of VSMCs (Figure 7A). Analysis of the ECM showed a decrease in relative elastin content of the media, as well as increased elastin fiber fragmentation in $Atg7^{F/F}$ SM22α-Cre^{+} mice as compared to

$Atg7^{+/+}$ SM22α-Cre^{+} mice (Figure 7B). No difference in relative collagen content was observed between the two groups ($Atg7^{+/+}$ SM22α-Cre^{+} vs. $Atg7^{F/F}$ SM22α-Cre^{+} segments: 35±3 vs. 41±8%, P> 0.05).

To identify the underling mechanism of ECM remodeling, the calcium binding protein, S100A4 which is known to regulate matrix remodeling via regulation of matrix metalloproteinase, expression was studied. The relative amount of S100A4 was significantly increased in aorta segments of $Atg7^{F/F}$ SM22α-Cre^{+} mice as compared to $Atg7^{+/+}$ SM22α-Cre^{+} mice (Figure 8).

3.4 Defective VSMC autophagy does not affect cardiac function

Stiffening of the aorta can have major implications for heart function, as increased stiffness leads to increased cardiac afterload and decreased diastolic coronary artery perfusion [38]. Although no differences were seen in ejection fraction, fractional shortening and left ventricular mass (Figure 9A-C), a trend towards a decreased stroke volume was observed in $Atg7^{F/F}$ SM22α-Cre^{+} mice as compared to $Atg7^{+/+}$ SM22α-Cre^{+} mice (Figure 9D). *In vivo* assessment of arterial stiffness by measurement of pulse wave velocity (PWV) did not reveal any significant differences between $Atg7^{F/F}$ SM22α-Cre^{+} and $Atg7^{+/+}$ SM22α-Cre^{+} mice.

4 Discussion

A decline of autophagy is an important feature of vascular aging since an age-related reduction of important autophagy markers have been demonstrated in both mice and humans [18, 19]. Although multiple studies indicate that induction of autophagy, either pharmacologically of via dietary adjustments, has considerable effects on arterial stiffness [10, 17, 18, 23, 24], mechanistic insights are still limited because the beneficial effects of these compounds or conditions are not solely dependent on autophagy and are also not limited to a specific cell type. Therefore, the aim of the present study was to investigate the specific role of VSMC autophagy on aortic stiffness and its biomechanical properties. In line with previous studies, we showed that autophagy plays an important role in the development of arterial stiffness, as a decrease in compliance was observed in aortic segments of mice with an autophagy deficiency in VSMCs. The increase in stiffness was most pronounced in passive unstimulated conditions and was highly pressure dependent. The pressure

dependency, which shows that differences in genotype are most noticeable at pressures exceeding normal physiological pressures, may be an explanation why, in contrast to *ex vivo* measurements, no differences were observed when measuring arterial stiffness by aortic PWV *in vivo*. In addition, the latter measurements were conducted under anesthesia, which by itself has an impact on vascular stiffness [35]. Moreover, there is a special variation in PWV, with the proximal aorta being more affected with age [33]. In the present study, *in vivo* measurements of PWV were conducted on the abdominal aorta while *ex vivo* measurements were performed in the thoracic aorta.

The most important ECM proteins defining passive aortic stiffness are elastin and collagen. Repetitive stretching of the aorta by the heart during every cardiac cycle will lead to material fatigue with progressive degradation and crosslinking of the ECM as a consequence. Because of the incredible long biological half-life of elastin (40 years), elastin degradation will not be repaired or replaced, leading to altered vessel wall biomechanics [41]. Accordingly, at normal pressures, when elastin is the load bearing component, loads will be transferred to the more rigid collagen and thus cause an increase in vascular stiffness [11]. Functional analysis of vascular remodeling was performed by using a wide pressure range, which includes an elastin/VSMC dependent region and a collagen-dependent region. The shifted pressure-dependency in the aortic segments from the $Atg7^{F/F}$ SM22α-Cre^{+} animals consistently remained after pharmacological removal of VSMC tone by DEANO, which provides strong evidence that macro- and/or micro-structural changes in the ECM were responsible for the observed differences in the intrinsic mechanical behavior of the aortic segments [22]. Indeed, although features of medial elastin fragmentation are normally observed only in aged vessels [16], autophagy deficiency in VSMCs accelerates the development of elastin degradation, as an increase in elastin breaks along with a decrease in total elastin was observed. Apart from ECM remodeling due to mechanical forces, matrix degradation can be induced by matrix metalloproteinase (MMP) produced by circulating cells, VSMCs or fibroblasts. The most abundant MMPs produced by VSMCs are MMP2 in physiological conditions, and MMP9 when cells are stimulated. MMP2 and MMP9 are responsible for the degradation of elastin, short collagens and degradation products of interstitial collagen [14]. Interestingly,

previous research with Atg7$^{F/F}$ SM22α-Cre^{+} mice showed that defective autophagy in VSMCs specifically promotes an upregulation of MMP9 and MMP2 [12]. In addition, autophagy inducer rapamycin decreases MMP2 and MMP9 in a rat model of thoracic aorta aneurism (TAA) [3], indicating a potential link between VSMC autophagy and matrix remodeling via regulation of MMPs. Ca^{2+} binding protein S100A4 was significantly increased in aortic segments of mice with VSMC autophagy deficiency. In line with our findings, it is reported that rapamycin normalizes increased S100A4 levels in aortas of a rat TAA model [3]. S100A4 is linked to inflammation and cancer metastasis by the disruption of the ECM [30, 36, 37]. Interestingly, when investigating rat thoracic aorta segments, spatiotemporal expression of S100A4, MMP2 and MMP9 were highly correlated, thereby indicating that S100A4 potentially acts as a regulator of MMP expression in the aorta [2]. In addition, S100A4 is directly linked to the phenotype of VSMC *in vitro* as well as *in vivo* [1, 4]. The mechanism by which autophagy deficiency in VSMCs alters passive aortic stiffness could be via S100A4 induced ECM remodeling. Besides changes in ECM composition, an increase in medial thickness was observed in Atg7$^{F/F}$ SM22α-Cre^{+} mice, which was in line with previous data [12]. Since the number of VSMCs was not changed, VSMC hypertrophy could be an explanation for the increased wall thickness in Atg7$^{F/F}$ SM22α-Cre^{+} mice. This is in line with *in vitro* data showing a hypertrophic phenotype of Atg7$^{F/F}$ SM22α-Cre^{+} VSMCs, which is characterized by cytosolic dilation and increased protein quantity [12]. However, also differences in ECM content, as indicated by changes in elastin and S100A4, can play a role in the increased aorta medial wall thickness.

The contribution of active modulators to the increased arterial stiffness in aortic segments of Atg7$^{F/F}$ SM22α-Cre^{+} mice was assessed by inducing contraction with the α_1- adrenergic receptor agonist phenylephrine (PE) in the presence or absence of eNOS inhibitor L-NAME. Previous evidence showed that (maximal) contraction of VSMCs has different effects on aortic biomechanics depending on the distention pressure. At pressures below 150 mmHg, VSMC contraction induces a decrease in compliance and an increase in Ep as compared to unstimulated conditions, while at pressures above 150 mmHg, VSMC contraction limits the pressure-dependent decrease in compliance and the increase in Ep [21]. This “stiffening” effect at low

pressures and “de-stiffening” effect at high pressures also occurred in the present study. However, the pressure by which the magnitude of VSMC contraction turns from stiffening to de-stiffening was significantly lower in $Atg7^{F/F}$ SM22α-Cre^{+} mice as compared to $Atg7^{+/+}$ SM22α-Cre^{+} mice, leading to the shift in differences between the groups to higher pressures under stimulated conditions. It is likely that this shift in increased arterial stiffness towards higher pressures is also a consequence of elastin degradation in $Atg7^{F/F}$ SM22α-Cre^{+} mice. In wild-type vessel segments, contraction of VSMCs at low to normal pressures will increase stiffness since it will result in the fractional unloading of the highly compliant elastin fibers. In mice with a VSMC-specific autophagy defect, however, degradation of elastin will cause collagen to bear a substantial amount of the wall stress, even at physiological pressures. Thus, increasing vascular tone to unload stiff collagen fibers will be beneficial. In addition, medial elastin degradation substantially affects collagen engagement properties which can explain the remaining difference in Ep even with VSMC contraction [11, 15].

Although previous research with $Atg7^{F/F}$ SM22α-Cre^{+} mice mainly showed differences in sensitivity to depolarization induced contractions [25], the present study mainly used α_1-receptor stimulation to induce contraction. However, we expected that the larger Ca^{2+} storage capacity in $Atg7^{F/F}$ SM22α-Cre^{+} VSMCs would indirectly affect α_1-receptor induced contractions. Even though differences between autophagy competent and deficient aortic segments shifted towards higher distention pressures with PE-induced contraction, no significant difference in the effect of PE between the groups was observed. Increased intracellular Ca^{2+} can alter a range of cellular functions besides VSMC contractility. Interestingly, changes in intracellular Ca^{2+} concentrations are involved in VSMC phenotype transition from a contractile to a proliferative/synthetic phenotype [27].

Increased arterial stiffness can have major consequences on the cardiovascular system. Because of a reduced capacity to dampen the pulsatile pulse evolving from left ventricular ejection, increased pulsatile energy will be transferred to the microcirculation with potential damage to high flow, low impedance organs such as the kidneys and brain. In addition, reflected pulse waves from the peripheral vascular system return earlier

in the cardiac cycle with increased systolic pressure and reduced coronary perfusion efficiency. An increased afterload during systole can have adverse effects on left ventricular function and remodeling, which can ultimately lead to heart failure [5]. While no differences were observed in ejection fraction or left ventricular mass, a trend towards a decreased stroke volume was observed in hearts of $Atg7^{F/F}$ SM22α-Cre^{+} mice. This propensity to a decreased stroke volume might be an initial response to the increased systolic load caused by arterial stiffness and can precede LV remodeling as a compensation mechanism to maintain cardiac output. Indeed, increased vascular load in humans, associated with aging, causes a decreased stroke volume and cardiac output [29]. In addition, overtraining-induced arterial stiffness is associated with a reduced stroke volume and cardiac output during exercise [6]. Also, in patients with type 1 diabetes, aortic stiffness is independently associated with stroke volume and cardiac output, yet also an association with ejection fraction has been observed [39].

Overall, we showed that autophagy in VSMCs is an important regulator of large artery stiffness. Blocking of autophagy in VSMCs resulted in aortic ECM remodeling, which directly affected passive arterial wall compliance. Since large artery stiffness is an important risk factor for cardiovascular disease, autophagy may act as a therapeutic target for effective treatment of these diseases.

5 Acknowledgements

The authors are grateful to Rita Van den Bossche, Hermine Fret, Nick Bakker and Geoffrey De Laender for excellent technical support, and Dr. Bronwen Martin for critical reading of the manuscript.

6 Funding

This work was supported by the Fund for scientific Research (FWO)-Flanders (grant N° G.0412.16N), the Hercules Foundation (grant number AUHA/13/03) and the University of Antwerp (BOF). D.G. De Munck is a fellow of the FWO-Flanders.

7 Autors' contributions

D.D.M., A.J.A.L and P.F. conception and design of research. D.D.M. and P.F. performed experiments. D.D.M. analyzed data, D.D.M. and P.F. interpreted results of experiments. D.D.M prepared the figures and drafted the manuscript, D.D.M., G.R.Y.D.M, W.M. and P.F. edited and revised the manuscript. D.D.M, A.J.A.L, G.R.Y.D.M, W.M. and P.F. approved the final version of the manuscript

8 References

1. Brisset AC, Hao H, Camenzind E, Bacchetta M, Geinoz A, Sanchez J-C, Chaponnier C, Gabbiani G, Bochaton-Piallat M-L (2007) Intimal smooth muscle cells of porcine and human coronary artery express S100A4, a marker of the rhomboid phenotype in vitro. Circ Res 100:1055–62. doi: 10.1161/01.RES.0000262654.84810.6c

2. Cao J, Geng L, Wu Q, Wang W, Chen Q, Lu L, Shen W, Chen Y (2013) Spatiotemporal Expression of Matrix Metalloproteinases (MMPs) is Regulated by the Ca2+-Signal Transducer S100A4 in the Pathogenesis of Thoracic Aortic Aneurysm. PLoS One 8. doi: 10.1371/journal.pone.0070057

3. Cao J, Wu Q, Geng L, Chen X, Shen W, Wu F, Chen Y (2017) Rapamycin inhibits CaCl2-induced thoracic aortic aneurysm formation in rats through mTOR-mediated suppression of proinflammatory mediators. Mol Med Rep 16:1911–1919. doi: 10.3892/mmr.2017.6844

4. Chaabane C, Bochaton-Piallat M-L (2015) Extracellular S100A4 induces smooth muscle cell phenotypic transition mediated by RAGE. Biochim Biophys Acta - Mol Cell Res 1853:2144–2157. doi: 10.1016/J.BBAMCR.2014.07.022

5. Chirinos JA, Segers P, Hughes T, Townsend R (2019) Large-Artery Stiffness in Health and Disease: JACC State-of-the-Art Review. J Am Coll Cardiol 74:1237–1263. doi: 10.1016/j.jacc.2019.07.012

6. Coates AM, Millar PJ, Burr JF (2018) Blunted cardiac output from overtraining is related to increased arterial stiffness. Med Sci Sports Exerc 50:2459–2464. doi: 10.1249/MSS.0000000000001725

7. De Munck DG, De Meyer GRY, Martinet W (2020) Autophagy as an emerging therapeutic target for age-related vascular pathologies. Expert Opin Ther Targets 24:131–145. doi: 10.1080/14728222.2020.1723079

8. Dikic I, Elazar Z (2018) Mechanism and medical implications of mammalian autophagy. Nat Rev Mol Cell Biol 19:349–364. doi: 10.1038/s41580-018-0003-4

9. Di Lascio N, Stea F, Kusmic C, Sicari R, Faita F (2014) Non-invasive assessment of pulse wave velocity in mice by means of ultrasound images. Atherosclerosis 237:31–37. doi: 10.1016/J.ATHEROSCLEROSIS.2014.08.033

10. Donato AJ, Walker AE, Magerko KA, Bramwell RC, Black AD, Henson GD, Lawson BR, Lesniewski LA, Seals DR (2013) Life-long caloric restriction reduces oxidative stress and preserves nitric oxide bioavailability and function in arteries of old mice. Aging Cell 12:772–83. doi: 10.1111/acel.12103

11. Fonck E, Prod'hom G, Roy S, Augsburger L, Rüfenacht DA, Stergiopulos N (2007) Effect of elastin degradation on carotid wall mechanics as assessed by a constituent-based biomechanical model. Am J Physiol - Hear Circ Physiol 292:H2754–H2763. doi: 10.1152/ajpheart.01108.2006

12. Grootaert MO, da Costa Martins PA, Bitsch N, Pintelon I, De Meyer GRY, Martinet W, Schrijvers DM (2015) Defective autophagy in vascular smooth muscle cells accelerates senescence and promotes neointima formation and atherogenesis. Autophagy 11:2014–2032. doi: 10.1080/15548627.2015.1096485

13. Hansen M, Rubinsztein DC, Walker DW (2018) Autophagy as a promoter of longevity: insights from model organisms. Nat Rev Mol Cell Biol 19:579–593. doi: 10.1038/s41580-018-0033-y

14. Johnson C, Galis ZS (2004) Matrix metalloproteinase-2 and -9 differentially regulate smooth muscle cell migration and cell-mediated collagen organization. Arterioscler Thromb Vasc Biol 24:54–60.

doi: 10.1161/01.ATV.0000100402.69997.C3

15. Kochová P, Kuncová J, Švíglerová J, Cimrman R, Miklíková M, Liška V, Tonar Z (2012) The contribution of vascular smooth muscle, elastin and collagen on the passive mechanics of porcine carotid arteries. Physiol Meas 33:1335–1351. doi: 10.1088/0967-3334/33/8/1335

16. Lacolley P, Regnault V, Avolio AP (2018) Smooth muscle cell and arterial aging: basic and clinical aspects. Cardiovasc Res 114:513–528. doi: 10.1093/cvr/cvy009

17. LaRocca TJ, Gioscia-Ryan RA, Hearon CM, Seals DR (2013) The autophagy enhancer spermidine reverses arterial aging. Mech Ageing Dev 134:314–320. doi: 10.1016/J.MAD.2013.04.004

18. LaRocca TJ, Hearon CM, Jr., Henson GD, Seals DR (2014) Mitochondrial Quality Control and Age-Associated Arterial Stiffening. Exp Gerontol 78–82. doi: 10.1016/J.EXGER.2014.07.008

19. LaRocca TJ, Henson GD, Thorburn A, Sindler AL, Pierce GL, Seals DR (2012) Translational evidence that impaired autophagy contributes to arterial ageing. J Physiol 590:3305–3316. doi: 10.1113/jphysiol.2012.229690

20. Leloup AJA, Van Hove CE, Kurdi A, De Moudt S, Martinet W, De Meyer GRY, Schrijvers DM, De Keulenaer GW, Fransen P (2016) A novel set-up for the ex vivo analysis of mechanical properties of mouse aortic segments stretched at physiological pressure and frequency. J Physiol 594:6105. doi: 10.1113/JP272623

21. Leloup AJA, Van Hove CE, De Moudt S, De Meyer GRY, De Keulenaer GW, Fransen P (2019) Vascular smooth muscle cell contraction and relaxation in the isolated aorta: a critical regulator of large artery compliance. Physiol Rep 7:e13934. doi: 10.14814/phy2.13934

22. Leloup AJA, De Moudt S, Van Hove CE, Dugaucquier L, Vermeulen Z, Segers VFM, De Keulenaer GW, Fransen P (2018) Short-Term Angiotensin II Treatment Affects Large Artery Biomechanics and

Function in the Absence of Small Artery Alterations in Mice. Front Physiol 9:582. doi: 10.3389/fphys.2018.00582

23. Mattison JA, Wang M, Bernier M, Zhang J, Park S-S, Maudsley S, An SS, Santhanam L, Martin B, Faulkner S, Morrell C, Baur JA, Peshkin L, Sosnowska D, Csiszar A, Herbert RL, Tilmont EM, Ungvari Z, Pearson KJ, Lakatta EG, de Cabo R (2014) Resveratrol Prevents High Fat/Sucrose Diet-Induced Central Arterial Wall Inflammation and Stiffening in Nonhuman Primates. Cell Metab 20:183–190. doi: 10.1016/J.CMET.2014.04.018

24. McCarthy CG, Wenceslau CF, Calmasini FB, Klee NS, Brands MW, Joe B, Webb RC (2019) Reconstitution of autophagy ameliorates vascular function and arterial stiffening in spontaneously hypertensive rats. Am J Physiol Heart Circ Physiol 317:H1013–H1027. doi: 10.1152/ajpheart.00227.2019

25. Michiels CF, Fransen P, De Munck DG, De Meyer GRY, Martinet W (2015) Defective autophagy in vascular smooth muscle cells alters contractility and Ca 2+ homeostasis in mice. Am J Physiol Circ Physiol 308:H557–H567. doi: 10.1152/ajpheart.00659.2014

26. Michiels CF, Fransen P, De Munck DG, De Meyer GRY, Martinet W (2015) Defective autophagy in vascular smooth muscle cells alters contractility and Ca2+ homeostasis in mice. Am J Physiol - Hear Circ Physiol 308:H557–H567. doi: 10.1152/ajpheart.00659.2014

27. Misárková E, Behuliak M, Bencze M, Zicha J (2016) Excitation-contraction coupling and excitation-transcription coupling in blood vessels: their possible interactions in hypertensive vascular remodeling. Physiol Res 65:173–91

28. Mizushima N, Komatsu M (2011) Autophagy: Renovation of Cells and Tissues. Cell 147:728–741. doi: 10.1016/J.CELL.2011.10.026

29. Nichols WW, O'Rourke MF, Avolio AP, Yaginuma T, Murgo JP, Pepine CJ, Conti CR (1985) Effects of age on ventricular-vascular coupling. Am J Cardiol 55:1179–1184. doi: 10.1016/0002-9149(85)90659-9

30. Ošlejšková L, Grigorian M, Gay S, Neidhart M, Šenolt L (2008) The metastasis associated protein S100A4: A potential novel link to inflammation and consequent aggressive behaviour of rheumatoid arthritis synovial fibroblasts. Ann Rheum Dis 67:1499–1504. doi: 10.1136/ard.2007.079905

31. Ren J, Sowers JR, Zhang Y (2018) Metabolic Stress, Autophagy, and Cardiovascular Aging: from Pathophysiology to Therapeutics. Trends Endocrinol Metab 29:699–711. doi: 10.1016/j.tem.2018.08.001

32. Ren J, Zhang Y (2018) Targeting Autophagy in Aging and Aging-Related Cardiovascular Diseases. Trends Pharmacol Sci 39:1064–1076. doi: 10.1016/J.TIPS.2018.10.005

33. Rogers WJ, Hu YL, Coast D, Vido DA, Kramer CM, Pyeritz RE, Reichek N (2001) Age-associated changes in regional aortic pulse wave velocity. J Am Coll Cardiol 38:1123–1129. doi: 10.1016/S0735-1097(01)01504-2

34. Safar ME (2018) Arterial stiffness as a risk factor for clinical hypertension. Nat Rev Cardiol 15:97–105. doi: 10.1038/nrcardio.2017.155

35. Sehgel NL, Vatner SF, Meininger GA (2015) Smooth Muscle Cell Stiffness Syndrome-Revisiting the Structural Basis of Arterial Stiffness. Front Physiol 6:335. doi: 10.3389/fphys.2015.00335

36. Šenolt L, Grigorian M, Lukanidin E, Simmen B, Michel BA, Pavelka K, Gay RE, Gay S, Neidhart M (2006) S100A4 is expressed at site of invasion in rheumatoid arthritis synovium and modulates production of matrix metalloproteinases. Ann Rheum Dis 65:1645–1648. doi:

10.1136/ard.2005.047704

37. Sherbet G V. (2009) Metastasis promoter S100A4 is a potentially valuable molecular target for cancer therapy. Cancer Lett 280:15–30. doi: 10.1016/j.canlet.2008.10.037

38. Singam NS V., Fine C, Fleg JL (2019) Cardiac changes associated with vascular aging. Clin Cardiol 1–7. doi: 10.1002/clc.23313

39. VanElderen SGC, Brandts A, Westenberg JJM, Van Der Grond J, Tamsma JT, Van Buchem MA, Romijn JA, Kroft LJM, Smit JWA, De Roos A (2010) Aortic stiffness is associated with cardiac function and cerebral small vessel disease in patients with type 1 diabetes mellitus: Assessment by magnetic resonance imaging. Eur Radiol 20:1132–1138. doi: 10.1007/s00330-009-1655-4

40. Vlachopoulos C, Aznaouridis K, Stefanadis C (2010) Prediction of Cardiovascular Events and All-Cause Mortality With Arterial Stiffness. A Systematic Review and Meta-Analysis. J Am Coll Cardiol 55:1318–1327. doi: 10.1016/j.jacc.2009.10.061

41. Wagenseil JE, Mecham RP (2009) Vascular extracellular matrix and arterial mechanics. Physiol Rev 89:957–989. doi: 10.1152/physrev.00041.2008

Figure legends

Figure 1 Western blot analysis of Atg7, LC3-I and p62 in aortic segments of $Atg7^{+/+}$ $SM22\alpha\text{-}Cre^{+}$ (+/+) and $Atg7^{F/F}$ $SM22\alpha\text{-}Cre^{+}$ mice (F/F) (A) with quantification relatively expressed to β-actin (B). (n=4, each lane represents one mouse) Mann Whitney U test. *p<0.05

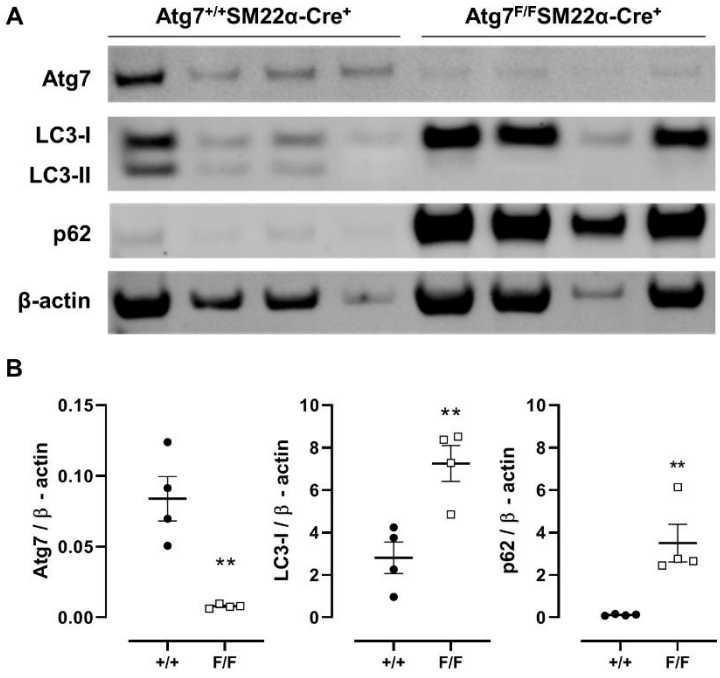

Figure 2 Pressure-dependency of diastolic diameter (A), compliance (B) and Ep (C) of $Atg7^{+/+}$ $SM22\alpha\text{-}Cre^{+}$ (+/+) and $Atg7^{F/F}$ $SM22\alpha\text{-}Cre^{+}$ (F/F) aortic vessel segments under control conditions (n=9-11). Pulse pressure was always 40 mmHg, hence each mean pressure point is ± 20 mmHg. Two-way ANOVA with Sidak post-hoc test. *p<0.05 **p<0.01 ***p<0.001

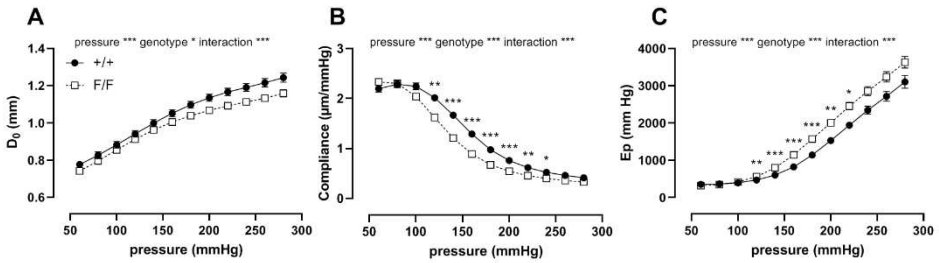

Figure 3 Differential effects of DEANO (vs Krebs-Ringer) on pressure-dependency of diastolic diameter (A), compliance (B) and Ep (C) of $Atg7^{+/+}$ SM22α-Cre^{+} (+/+) and $Atg7^{F/F}$ SM22α-Cre^{+} (F/F) aortic vessel segments in maximally relaxed conditions using 2 µM DEANO and (n=9-11). Pulse pressure was always 40 mmHg, hence each mean pressure point is ± 20 mmHg. Two-way ANOVA with Sidak post-hoc test. *p<0.05 **p<0.01 ***p<0.001

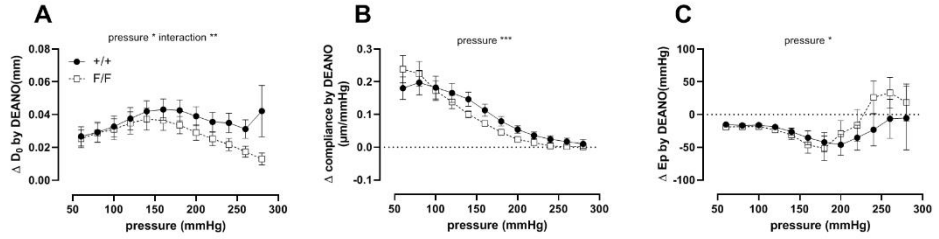

Figure 4 Differential effects of PE (vs Krebs-Ringer) on the pressure-dependency of diastolic diameter (A), compliance (B) and Ep (C) of $Atg7^{+/+}$ SM22α-Cre^{+} (+/+) and $Atg7^{F/F}$ SM22α-Cre^{+} (F/F) aortic vessel segments contracted with 2 µM PE and (n=9-11). Pulse pressure was always 40 mmHg, hence each mean pressure point is ± 20 mmHg. Two-way ANOVA with Sidak post-hoc test. ***p<0.001

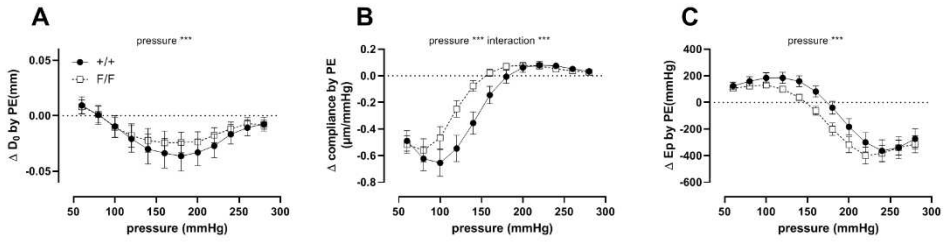

Figure 5 Differential effects of PE + L-NAME (vs Krebs-Ringer) on the pressure-dependency of diastolic diameter (A), compliance (B) and Ep (C) of $Atg7^{+/+}$ SM22α-Cre^{+} (+/+) and $Atg7^{F/F}$ SM22α-Cre^{+} (F/F) aortic vessel segments contracted with 2 μM PE + L-NAME and (n=9-11). Pulse pressure was always 40 mmHg, hence each mean pressure point is ± 20 mmHg. Two-way ANOVA with Sidak post-hoc test. ***p<0.001

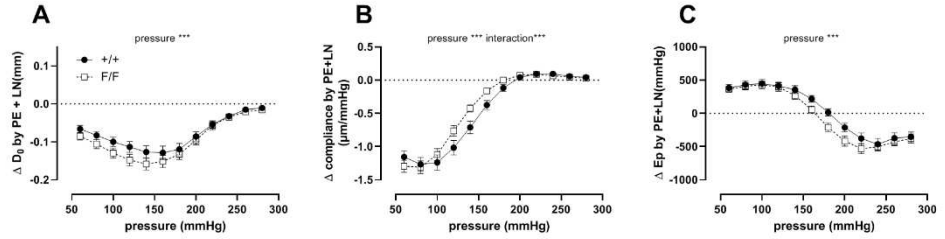

Figure 6 Pressure-dependency of Ep in unstimulated conditions (Krebs Ringer, KR) and after stimulation with 2 μM PE in the absence or presence of 300 μM L-NAME (LN) in $Atg7^{+/+}$ SM22α-Cre^{+} (+/+) (A) and $Atg7^{F/F}$ SM22α-Cre^{+} mice (F/F) (C) and absolute change from baseline (KR) (B and D) are displayed. E and F display respectively intersect with the x-axis by PE and PE+LN. (n=9-11) Unpaired student t-test. *p<0.05.

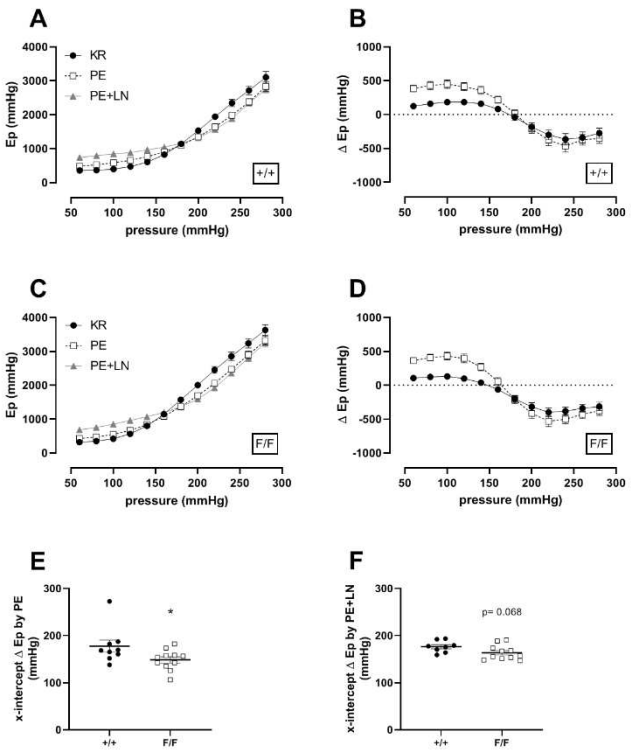

Figure 7 Important wall structure parameters of aortic segments of $Atg7^{+/+}$ SM22α-Cre^{+} (+/+) and $Atg7^{F/F}$ SM22α-Cre^{+} mice (F/F) (A) Hematoxylin and eosin staining and quantification of wall thickness and number of VSMCs per µm² surface area. (B) Orcein staining and quantification of relative amount of elastin and elastin breaks. (n=7-10) Unpaired student t-test. *p<0.05. Scale bar: 100 µm

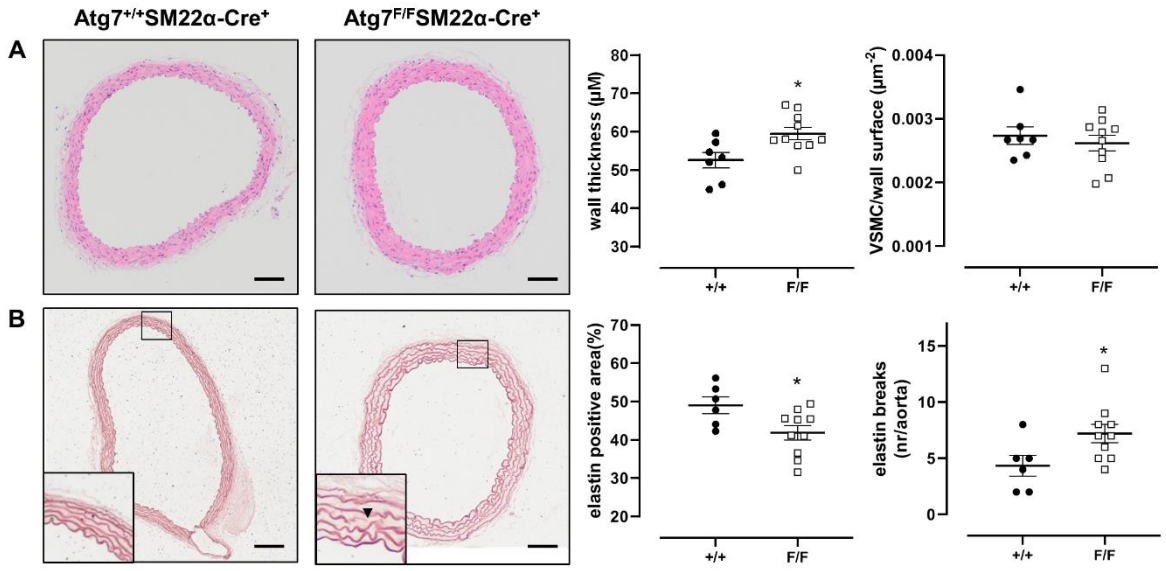

Figure 8 Immunohistochemical staining of S100A4 in aorta segments of Atg7$^{+/+}$ SM22α-Cre^{+} (+/+) and Atg7$^{F/F}$ SM22α-Cre^{+} (F/F) mice. (n=7-10) Unpaired student t-test. **p<0.01. Scale bar: 100 µm

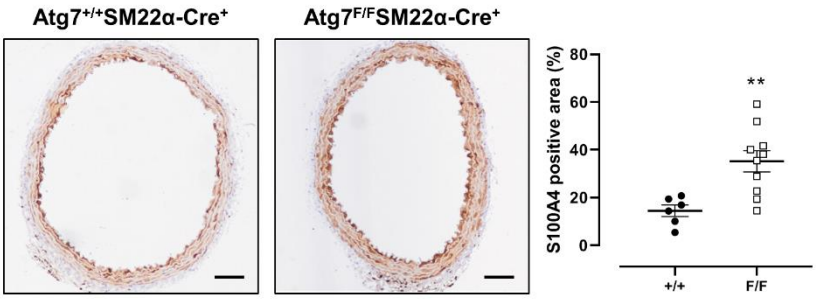

Figure 9 Ejection fraction (EF), Fractional shortening (FS), Pulse wave velocity (PWV), Left ventricular mass (LVmass) and stroke volume of Atg7$^{F/F}$ SM22α-Cre^{+} mice (F/F) as compared to Atg7$^{+/+}$ SM22α-Cre^{+} mice. (N=7-11) Unpaired Student t-test.

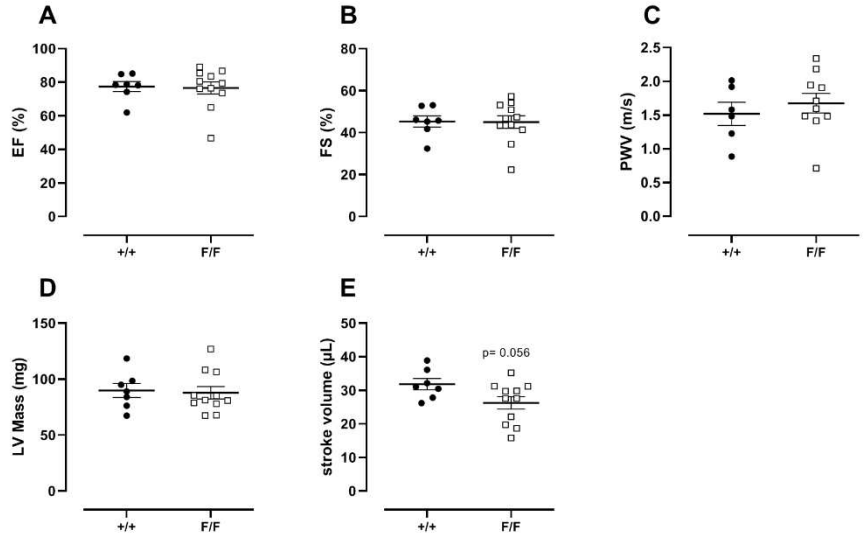
A
EF (%)
100
80
60
40
20
0
+/+
F/F
B
FS (%)
80
60
40
20
0
+/+
F/F
C
PWV (m/s)
2.5
2.0
1.5
1.0
0.5
0.0
+/+
F/F
D
LV Mass (mg)
150
100
50
0
+/+
F/F
E
stroke volume (µL)
50
40
30
20
10
0
p= 0.056
+/+
F/F